**Atmospheric
Chemistry
and Physics
Discussions**

Size-distributions of *n*-hydrocarbons, PAHs and hopanes and their sources in the urban, mountain and marine atmospheres over East Asia

G. Wang[1,2,3], K. Kawamura[2], M. Xie[3], S. Hu[3], S. Gao[3], J. Cao[1], Z. An[1], and Z. Wang[4]

[1]State Key Laboratory of Loess and Quaternary Geology, Institute of Earth Environment, Chinese Academy of Sciences, Xi'an 710075, China
[2]Institute of Low Temperature Science, Hokkaido University, Sapporo 060-0819, Japan
[3]School of the Environment, State Key Laboratory of Pollution Control and Resources Reuse, Nanjing University, Nanjing 210093, China
[4]Institute of Atmospheric Physics, Chinese Academy of Sciences, Beijing 100029, China

**Size-distributions of
n-hydrocarbons,
PAHs and hopanes
and their sources**

G. Wang et al.

Title Page

Abstract	Introduction
Conclusions	References
Tables	Figures

|◄ | ►|

◄ | ►

Back | Close

Full Screen / Esc

Printer-friendly Version

Interactive Discussion

Abstract

Size-segregated (9 stages) *n*-alkanes, polycyclic aromatic hydrocarbons (PAHs) and hopanes in the urban (Baoji city in inland China), mountain (Mt. Tai in east coastal China) and marine (Okinawa Island, Japan) atmospheres over East Asia were stud-
5 ied using a GC/MS technique. Concentrations of *n*-alkanes (1698±568 ng m^{-3} in winter and 487±145 ng m^{-3} in spring), PAHs (536±80 and 161±39 ng m^{-3}), and hopanes (65±24 and 20±2.4 ng m^{-3}) in the urban air are 1–2 orders of magnitude higher than those in the mountain aerosols and 2–3 orders of magnitude higher than those in the marine samples. Mass ratios of *n*-alkanes, PAHs and hopanes clearly demonstrate
10 coal-burning emissions as the major source of the determined organic aerosols. Size distributions of fossil fuel derived *n*-alkane, PAHs and hopanes were found as a unimodal in most cases, peaking at 0.7–1.1 µm size. In contrast, plant wax derived *n*-alkanes present a bimodal distribution with two peaks at the sizes of 0.7–1.1 µm and >4.7 µm in the summer mountain and spring marine samples. Among the three types
15 of samples, geometric mean diameter (GMD) of the determined organics in fine mode (<2.1 µm) was the smallest (av. 0.63 µm in spring) in the urban samples and the largest (1.01 µm) in the marine samples, whereas the GMD in coarse mode (≥2.1 µm) was smallest (3.48 µm) in the marine aerosols and largest (4.04 µm) in the urban aerosols. The fine mode of GMDs in the urban and mountain samples were larger in winter than
20 in spring and summer. Moreover, GMDs of 3- and 4-ring PAHs were larger than 5- and 6-ring PAHs in the three types of atmospheres. Such differences in GMDs may be interpreted by coagulation and repartitioning of organic compound during a long range transport from the inland continent to the marine site, suggesting that the size changes arising from these physical processes must be included in climate models in relevant
25 to organic aerosols.

1   Introduction

Atmospheric aerosols influence climate directly by scattering and absorbing radiation, and indirectly by modifying the optical properties and lifetime of clouds via acting as cloud condensation nuclei (Albrecht, 1989; Ramanathan, 2001). Airborne particles contain toxic matters such as heavy metals and organic pollutants, thus are deeply linked with human health (Dockery et al., 1993; Finlayson-Pitts and Pitts Jr., 2000; Anderson, 2009). Organic compounds constitute a substantial fraction of atmospheric aerosols. Especially for fine particles less than 2 µm in diameter, 20–90% of the mass is carbonaceous (Seinfeld and Pankow, 2003; Kanakidou et al., 2005).

Aerosol sources in East Asia are different from those in Europe and North America, because much more coal and biomass are burned with minimal emission controls in some cases, adding more absorbing soot and organic aerosol to the Asian and Pacific atmosphere (Aldhous, 2005; Arimoto et al., 2006). Economic expansion in China causes an increase in the amount of SO_2, organic matter, and soot emitted into the East Asia atmosphere (Akimoto, 2003; Huebert et al., 2003). The frequent presence of desert dust makes the East Asian atmosphere more complex by scattering sunlight back to space and absorbing solar and terrestrial radiation (Huebert et al., 2003). Moreover, the dust also serves as an alkaline surface for the uptake of acidic gases. Sharp industrialization and urbanization in China result in the atmospheric level of nitrogen dioxide higher than that in Europe and North America (Akimoto, 2003), thus the oxidizing environment of the East Asian atmosphere is likely being changed.

Physical properties of atmospheric aerosols depend on their chemical compositions and sizes (Seinfeld and Pandis, 1998; Hinds, 1999; Kanakidou et al., 2005). These airborne particles cover a wide range of sizes from a few nanometers to several hundreds of micrometers, commonly a hundredfold range between the smallest and the largest particles of an aerosol (Seinfeld and Pandis, 1998; Finlayson-Pitts and Pitts Jr., 2000). Numerous studies have demonstrated that chemical and physical properties of atmospheric aerosols including abundances, composition and size distributions are area-

and location-specific (Pierce and Katz, 1975; Venkataraman et al., 1994; Kleeman and Cass, 1999; Kleeman et al., 1999; Venkataraman et al., 2002; Kleeman et al., 2008; Riddle et al., 2008). Few studies on size distributions of organic aerosols are sparsely conducted for *n*-alkanes, PAHs and carboxylic acids in economically developed coastal
5 cities in China such as Hong Kong (Yu et al., 2004; Huang et al., 2006; Zheng et al., 2008), Guangzhou (Bi et al., 2005; Duan et al., 2007) and Beijing (Yao et al., 2003). However, there is no such study from inland China.

   In order to investigate the similarity and differences in the chemical compositions and size distributions of different types of aerosols from different atmospheric environments
10 in East Asia, we have characterized size-segregated atmospheric particles from Baoji (an inland Chinese city), Mt. Tai (China) and Okinawa Island (Japan). In the current paper we first present concentrations, compositions, and sources of particulate organic compounds (i.e., *n*-alkanes, PAHs and hopanes) in the three types of atmospheric environments, and then characterize their detailed size distributions on a molecular
15 level.

2   Experimental section

2.1   Sample collection

Baoji is a mid-scale city located in central China with a population of 0.75 million (Fig. 1). The sampler was set on the rooftop of a three-floor building at the Envi-
20 ronment Monitoring Station of Baoji, which is in the urban center. Winter sampling was performed on 11–14 January and 12–20 February 2008, while spring sampling was conducted on 12–24 April 2008. Size-segregated mountain aerosols were collected on the mountaintop (elevation of 1534 m a.s.l.) of Mt. Tai located in the central North China Plain, which faces to the East China Sea, Korean Peninsula and Japanese Islands. The
25 mountain sampling was performed for 7 d (22–29 June 2006) in the summer and 12 d (12–24 January 2008) in the winter on the square in front of the Meteorological Station

located in the mountaintop. Size-segregated marine aerosols were collected from 18 March to 12 April 2008 at Cape Hedo of Okinawa Island, Japan (Fig. 1). There is no major industry in the island, and local anthropogenic activities are insignificant. Thus air pollution from the local sources is negligible.

Size-segregated aerosols at the urban and mountain sites were collected by Andersen 8-stage air samplers (Thermoelectronic Company, USA) with the same cutoff sizes 9.0, 5.8, 4.7, 3.3, 2.1, 1.1, 0.7, and 0.4 µm at an airflow rate of 28.3 L min^{-1}. On the other hand, the marine size-resolved aerosols were collected by another type of Andersen 8-stage sampler (Tokyo Dylec Company, Japan) at a flow rate of 100 L min^{-1} with cutoff sizes as 11.3, 7.0, 4.7, 3.3, 2.1, 1.1, 0.7, and 0.4 µm. All the collected samples were stored at −20°C before analysis. Information including dates, sample numbers, sampling durations and particle concentrations is shown in Table 1.

2.2 Sample extraction, derivatization and GC/MS analysis

Detailed methods for extraction, derivatization and gas chromatography/mass spectrometer (GC/MS) analysis are described elsewhere (Wang et al., 2006). Briefly, aliquots of the sample and blank filters were extracted with a mixture of dichloromethane and methanol (2:1) under ultrasonication. The extracts were concentrated using a rotary evaporator under vacuum and then dried under a pure nitrogen stream. After converting polar compounds into non-polar ones through a reaction with BSTFA, the extracts were diluted with n-hexane prior to GC/MS determination.

GC/MS analysis of the derivatized fraction was performed using a Hewlett-Packard 6890 GC coupled to a Hewlett-Packard 5973 MSD. The GC separation was carried out on a DB-5MS fused silica capillary column with the GC oven temperature programmed from 50°C (2 min) to 120°C at 15°C min^{-1} and then to 300°C at 5°C min^{-1} with final isothermal hold at 300°C for 16 min. The sample was injected in a splitless mode at an injector temperature of 280°C, and scanned from 50 to 650 Da using electron impact (EI) mode at 70 eV. GC/MS response factors were determined using authentic standards. Average recoveries of the target compounds were better than 80%. No serious

Size-distributions of n-hydrocarbons, PAHs and hopanes and their sources

G. Wang et al.

contamination was found in the field blanks. Here we report on the non-polar compounds (i.e., n-alkanes, PAHs and hopanes) to discuss the differences in their molecular compositions, size distributions and sources in the three types of atmospheres, while the polar compounds such as sugars and carboxylic acids will be presented in a forthcoming paper.

3 Results and discussion

3.1 Abundances and molecular compositions

Concentrations of individual compounds in all the impactor stages are summed and average concentrations are shown in Table 2 as total suspended particle (TSP)-equivalent concentrations. The TSP-equivalent concentrations of the compounds determined in Baoji city are 1–2 orders of magnitude higher than those in the mountain samples and 2–3 orders of magnitude higher than those in the marine samples. Compared with those in Chinese mega-cities (Wang et al., 2006), concentrations of n-alkanes and PAHs in Baoji are comparable or even higher than those in the heavily polluted mega-cities like Xi'an and Chongqing, suggesting that air pollutions in mid-scale Chinese cities are also very severe.

3.1.1 *n*-Alkanes

Homologues (C_{18}–C_{36}) of n-alkanes were detected in the urban, mountain and marine aerosols with different concentration levels and molecular compositions (Table 2 and Fig. 2). In the urban samples, total n-alkanes in all the nine stages are $1698\pm568\,\mathrm{ng\,m^{-3}}$ in winter and $487\pm145\,\mathrm{ng\,m^{-3}}$ in spring with a major peak at C_{23}/C_{25} and a minor peak at C_{31} (Fig. 2a and b). In contrast, the total concentrations were found to be much lower in the mountain ($126\pm88\,\mathrm{ng\,m^{-3}}$ in winter and $41\,\mathrm{ng\,m^{-3}}$ in summer) and marine atmospheres ($7.9\pm6.1\,\mathrm{ng\,m^{-3}}$ in spring) with a major peak at C_{29}/C_{31} and

a relatively minor predominance in a range of C_{23}–C_{27} (Fig. 2c–e). Baoji is an inland city located in the economically developing region of China, where coal usage accounts for more than 95% of the energy consumption. The local severe air pollution in winter is mainly due to emissions from coal burning with low efficiency for house heating,

5 although the winter stagnant conditions favor the pollutant accumulation.

Plant wax derived *n*-alkanes have odd-number carbon predominance with a carbon preference index (CPI, odd/even) of >5, whereas CPI of fossil fuel derived *n*-alkanes is close to unity (Rogge et al., 1993b; Simoneit et al., 2004a). As seen in Table 3, CPI values are close to unity for the urban and mountain samples in winter and spring,

10 suggesting an importance of major contribution from anthropogenic activities such as domestic coal burning and petroleum combustion. The CPI values increase to around 2 for the mountain samples in summer and the marine samples in spring, indicating an enhanced biogenic input in those regions.

3.1.2 PAHs

15 In the urban area, TSP-equivalent concentrations of total PAHs were found to be 536 ± 80 ng m^{-3} in winter and 161 ± 39 ng m^{-3} in spring, which are 10 times higher than those of the mountain samples and 250 times higher than those of the marine samples (Table 2). Benzo(b/k)fluoranthene (BbkF) is the dominant PAH in all the samples (Fig. 3 and Table 2), accounting for 17–62% of the total PAHs. The second most abundant PAH

20 in the urban area is dibenzo(a,e)pyrene (DBP) (Fig. 3a and b), whose concentrations are 54 ± 24 and 19 ± 6.5 ng m^{-3} during winter and spring, respectively. Conversely, the second most abundant PAH in the mountain and marine samples is fluoranthene (Flu) (Fig. 3c–e). Such a difference in the molecular composition of PAHs may be related to the differences in their sources and atmospheric processes (e.g., condensation and

25 decomposition) during a long-range transport.

Diagnostic ratios of PAHs are indicative of their sources. For examples, concentration ratios of indeno(1,2,3-cd)pyrene to benzo(ghi)perylene (IP/BghiP) are 0.2, 0.5 and 1.3 in the smokes from gasoline, diesel and coal combustions (Grimmer et al., 1983),

whereas the ratios of benzo(ghi)perylene to benz(e)pyrene (BghiP/BeP) are 2.0 and 0.8 in the mobile exhausts and coal burning emissions, respectively (Ohura et al., 2004). As shown in Table 3, IP/BghiP and BghiP/BeP ratios in the urban, mountain and marine samples are close to those in coal burning smokes, suggesting that PAHs
5 in the East Asia aerosols are largely derived from coal combustions, being consistent with the particulate PAHs compositions previously reported for 14 Chinese cities (Wang et al., 2006).

3.1.3 Hopanes

Hopanes are triterpenoid hydrocarbons that are primarily derived from bacteria as bac-
10 teriohopanols and produced by diagenesis in sediments over a geological time (Oros and Simoneit, 1999). They are abundant in coal and crude oils and enriched in lubricant oil fraction (Kawamura et al., 1995). A series of hopanes were detected in the urban samples with total concentrations of 65±24 and 20±2.4 ng m^{-3} in winter and spring, respectively (Table 2). Concentrations of hopanes in the mountain samples are about
15 two orders of magnitude lower than those in the urban Baoji samples, while hopanes in the marine samples are undetectable. Molecular composition of hopanes in the urban aerosols are characterized by one peak at 17β(H),21α(H)-30-norhopane (C$_{29\beta\alpha}$) in winter and by two peaks at 17α(H),21β(H)-30-norhopane (C$_{29\alpha\beta}$) and 17α(H),21β(H)-30-hopane (C$_{30\alpha\beta}$) in spring (Fig. 4a and b). Their dominations are different from those
20 of the mountaintop samples, which are dominated by two major congeners (C$_{29\alpha\beta}$ and C$_{30\alpha\beta}$) in winter and one major congener (C$_{30\alpha\beta}$) in summer (Fig. 4c and d).
  Such differences in the molecular compositions of hopanes can be further assessed by their mass ratios. As shown in Table 3, diagnostic ratios of hopanes in the urban samples in winter fall in the range of coal burning emissions but shift toward the range
25 of traffic emissions in spring when domestic coal burning for house heating is shut down in China. With respect to the mountain samples, we also found that hopane diagnostic ratios are more indicative of coal burning smoke in winter than in summer. However, the wintertime ratios in the mountain samples are less indicative of coal combustion

emissions compared to those in the urban samples. Mt. Tai is located in the east coastal China, where economy is more developed than that in inland cities like Baoji and traffic pollution is much more significant (Akimoto, 2003; Wang et al., 2007). Thus contributions of mobile emissions to hopanes are pronounced in the mountain region
₅ especially in summer (Table 3).

3.2 Size distributions

Abundances of the three classes of compounds in each impactor stage are presented in Table 4, together with their cumulative percentages calculated. Wintertime cumulative percentages of n-alkanes (86%, Table 4), PAHs (93%) and hopanes (90%) in urban
₁₀ fine particles (<2.1 μm) are higher than those (80%, 85% and 82% for n-alkanes, PAHs and hopanes, respectively, Table 4) in the mountain fine particles. Further, their springtime cumulative percentages (77% and 94% for n-alkanes and PAHs, Table 4) in the urban (Baoji) fine particle are also higher than those (65% and 87% for n-alkanes and PAHs) in the marine fine particles, suggesting that compared to those in the mountain
₁₅ and marine samples n-alkanes, PAHs and hopanes are enriched in smaller particles in the urban air. Detailed differences in their size distributions among the three types of samples are further discussed as below.

3.2.1 *n*-Alkanes

To better understand the differences in size distributions of n-alkanes from natural and
₂₀ anthropogenic sources, total n-alkanes in each impactor stage were differentiated as plant wax and fossil fuel derived n-alkanes using the method described by Simoneit et al. (2004a). Concentrations of the two classes of n-alkanes and CPI values of the total n-alkanes are plotted in Fig. 5 as a function of particle sizes.
   In the urban atmosphere both fossil fuel derived and plant wax derived n-alkanes
₂₅ showed a unimodal size distribution in winter and spring with maximal concentrations at range of 0.7–1.1 μm (Fig. 5a and b). With respect to the mountain samplers, the two

classes of *n*-alkanes present a unimodal size distribution in winter with concentration maxima at the sizes of 0.7–1.1 µm and 1.1–2.1 µm, respectively (Fig. 5c). Although a bimodal size distribution was found for both types of *n*-alkanes in the mountain summer aerosols (Fig. 5d), the fossil fuel derived *n*-alkanes present a major peak in the size of 0.7–1.1 µm and a minor peak in the size of 4.7–5.8 µm while the plant wax derived *n*-alkanes present two equivalent peaks at the same size ranges. A bimodal distribution was observed for the two types of *n*-alkanes in the marine aerosols with a maximum in the submicrometer size of 0.7–1.1 µm, followed by a small peak in supermicrometer size of >9.0 µm, but their mass concentrations in submicrometer size (<1.1 µm) are less than those in the urban and mountain aerosol samples (Fig. 5e and Table 4).

CPI values are close to unity in the backup filters and generally increase with an increase in particle sizes for all samples (Fig. 5a–e), except for the sample sets collected in the wintertime from the urban site (Fig. 5a), indicating a predominance of fossil fuel-derived *n*-alkanes in the smallest size and an increasing input of plant wax derived *n*-alkanes along with an increase in particle sizes. The decreased CPI value in the wintertime urban aerosol particles >3.3 µm (Fig. 5a) was mostly caused by the decreased relative abundance of biogenic *n*-alkanes in the coarse fraction probably due to the deposition of large particles under the stagnant conditions.

3.2.2 PAHs

PAHs in all the samples were found with a unimodal distribution peaking in fine mode (<2.1 µm) in the whole size ranges except for 3- and 4-ring PAHs in the summer mountain aerosols (Fig. 6a–e). In the urban aerosols, all the determined PAHs maximized at the range 0.7–1.1 µm in winter and spring (Fig. 6a and b), but the second highest peak was found in a larger size 1.1–2.1 µm during winter and in a smaller size 0.4–0.7 µm during spring. In the mountain region, all the PAH concentrations maximized in the ranges of 0.7–1.1 µm and 1.1–2.1 µm during winter and summer (Fig. 6c and d), but 3- and 4-ring PAHs showed a minor peak at the size 4.7–5.8 µm during summer (Fig. 6d),

probably caused by the enhanced adsorption of gaseous 3- and 4-ring PAHs on coarse particles in the hot season. As seen in Fig. 6e, all the PAHs showed two equivalent peaks in the sizes of 0.7–1.1 and 1.1–2.1 µm, suggesting a significant migration toward larger particles compared to those in the urban atmosphere during the same season.

5 In general, relative abundances of 3- and 4-ring PAHs to 5- and 6-ring PAHs are lower in small particles and higher in large particles in the three types of the atmospheres during different seasons (Fig. 6a–e). Lower molecular weight (LMW) PAHs in solid phase can evaporate into the air and subsequently adsorb/condense onto pre-existing particles. Such a repartitioning effect makes semi-volatile PAHs more likely shift to the

10 larger particles than the less volatile PAHs (Offenberg and Baker, 1999).

3.2.3 Hopanes

$C_{29\alpha\beta}$ and $C_{30\alpha\beta}$ are the two major hopane species detected in the urban and mountain samples, which we selected here to discuss the difference of size distributions of hopanes in the atmosphere during different seasons. The two hopanes showed a sim-

15 ilar size distribution in the urban and mountain samples (Fig. 7a–d). This is reasonable because these congeners have common origins with similar molecular weight and are thus have similar behavior in the atmosphere. In the urban winter aerosols, they are characterized by a unimodal distribution with a peak in the 0.7–1.1 µm size range (Fig. 7a). In contrast, they showed a bimodal distribution in spring with a major peak at

20 size of 0.7–1.1 µm and a minor peak at size of 3.3–4.7 µm (Fig. 7b). In the wintertime mountain samples, the two hopanes displayed a unimodal distribution with a maximum in the 0.7–1.1 µm size (Fig. 7c), whereas they showed a bimodal distribution in summer with two peaks at the ranges of 0.7–1.1 µm and >3.3 µm sizes (Fig. 7d).

3.3 Geometric mean diameters (GMD) in the fine and coarse modes

25 In order to better characterize the spatial and seasonal differences in size distributions of the determined organic compounds in the East Asia atmosphere, we calculated

their GMDs for the fine (<2.1 µm) and coarse (≥2.1 µm) modes and the whole range of impactor particle sizes (see Table 5). *n*-Akanes, PAHs and hopanes in all the samples mostly originated from fossil fuel combustions, and thus centered in fine particles (Keshtkar and Ashbaugh, 2007), leading to their total GMDs in the whole range of impactor sizes very close to the fine mode ones. Among the three sampling sites the fine and the total GMDs of all the compounds are smallest in the urban air and largest in the marine atmosphere, which is most likely due to the enhanced repartitioning of organics during a long-range transport. In contrast, GMDs of fossil fuel-derived *n*-alkanes, PAHs and hopanes in coarse mode are largest in the urban area and smallest in the marine region, suggesting the increased deposition during the transport from lowlands to mountaintop and from inland continent to marine. However, wintertime GMDs (3.91±0.68 µm, Table 5) of the plant wax-derived *n*-alkanes in coarse mode in the mountain air are larger than those (3.54±0.08 µm) in the urban atmosphere mainly due to an increased input by wind abrasion with local plant surface, while springtime GMDs (3.92±0.23 µm, Table 5) of the plant wax-derived *n*-alkanes in coarse mode in the marine samples are smaller than those (4.38±0.27 µm) in the urban samples mainly due to an enhanced deposition during a long range transport.

In the urban region, GMDs of all the compounds in fine mode are larger in winter than in spring, being opposite to those of the coarse mode (see Table 5 for the numbers). A similar trend was also found for the mountain samples between winter and summer seasons. Such seasonal variations can be explained firstly by the differences in the sources and secondly by the increased effects of fine particle coagulation, organic compound repartitioning and coarse particle deposition in winter due to the inversion layer development (Herner et al., 2006). PAHs are produced by incomplete combustion of carbon-containing materials. Less volatile HMW PAHs are predominantly formed on smaller particles where they condense immediately after the emission of combustion products while more volatile LMW PAHs are adsorbed on larger particles when the smoke is cooled down in the ambient air. Furthermore, solid-phase LMW PAHs can evaporate into the gas phase and re-adsorb/condense on pre-existing particles (Offen-

berg and Baker, 1999). Thus compared to HMW (5- and 6-ring) PAHs, LMW (3- and 4-ring) PAHs may show larger GMDs for all the samples (Table 5). This repartitioning of semivolatile PAHs can be enhanced under higher ambient temperature, leading to an increase in the ratios of total GMDs of LMW PAHs to total GMDs of HMW PAHs in warm periods: a shift from 1.16 in winter to 1.27 in spring for the urban samples and from 1.15 in winter to 1.22 in summer for the mountaintop samples.

4 Summary and conclusion

n-Alkanes, PAHs and hopanes were determined on a molecular level in size-segregated aerosols from the urban (Baoji), mountain (Mt. Tai) and marine (Okinawa Is.) sites over East Asia for different seasons. Winter and spring concentrations of n-alkanes, PAHs and hopanes in the urban aerosols are 1698±568 and 487±145 ng m^{-3}, 536±80 and 161±39 ng m^{-3} and 65±24 and 20±2.4 ng m^{-3}, respectively. These values are 1–2 and 2–3 orders of magnitude higher than those of the mountain and marine aerosols, respectively. Concentration ratios and compositions of the organics determined indicate that coal combustion in China is the major source of airborne PAHs in the aerosols over East Asia.

Size distributions of fossil fuel derived n-alkanes, PAHs and hopanes were generally found as unimodal with a peak at the particle size less than 2.1 μm in all the samples. In contrast, plant wax derived n-alkanes in the summer mountain and spring marine aerosols present a bimodal size distribution with two peaks at the size ranges of 0.7–1.1 μm and >4.7 μm probably by the increased input due to mechanical processes like wind abrasion on plant leaves and ground surfaces. Based on the calculation of the GMDs of organic compounds in the three types of atmospheres, we found that fossil fuels derived n-alkanes, PAHs and hopanes in the urban aerosols are mostly present in smallest sizes whereas those of the marine aerosols are mostly in the largest sizes. Moreover, their sizes are larger in winter than in spring and summer. Such spatial and seasonal differences in the sizes may be most likely caused by coagulation of fine

Full Screen / Esc

Printer-friendly Version

Interactive Discussion

particles and repartitioning of organic compounds in addition to the differences in their sources. Particle sizes of 3- and 4-ring PAHs are larger than those of 5- and 6-ring PAHs in all the sample sets due to more significant repartitioning of the former PAHs. Such a repartitioning can be enhanced under higher ambient temperatures in summer than in winter, causing a migration of LMW PAHs toward large particles.

References

Akimoto, H.: Global air quality and pollution, Science, 302, 1716–1719, 2003.

Albrecht, B. A.: Aerosols, cloud microphysics, and fractional cloudiness, Science, 245, 1227–1230, 1989.

Aldhous, P.: China's burning ambition, Nature, 435, 1152–1154, 2005.

Anderson, H. R.: Air pollution and mortality: A history, Atmos. Environ., 43, 142–152, 2009.

Arimoto, R., Kim, Y. J., Kim, Y. P., Quinn, P. K., Bates, T. S., Anderson, T. L., Gong, S., Uno, I., Chin, M., Huebert, B. J., Clarke, A. D., Shinozuka, Y., Weber, R. J., Anderson, J. R., Guazzotti, S. A., Sullivan, R. C., Sodeman, D. A., Prather, K. A., and Sokolik, I. N.: Characterization of Asian Dust during ACE-Asia, Global Planet. Change, 52, 23–56, 2006.

Bi, X., Sheng, G., Peng, P., Chen, Y., and Fu, J.: Size distribution of *n*-alkanes and polycyclic aromatic hydrocarbons (PAHs) in urban and rural atmospheres of Guangzhou, China, Atmos. Environ., 39, 477–487, 2005.

Dockery, D. W., Pope, C. A., Xu, X., Spengler, J. D., Ware, J. H., Fay, M. E., Ferris Jr., B. G., and Speizer, F. E.: An association between air pollution and mortality in six U.S. cities, New Engl. J. Med., 329, 1753–1759, 1993.

Duan, J. C., Bi, X. H., Tan, J. H., Sheng, G. Y., and Fu, J. M.: Seasonal variation on size distribution and concentration of PAHs in Guangzhou city, China, Chemosphere, 67, 614–622, 2007.

Finlayson-Pitts, B. J. and Pitts Jr., J. N.: Chemistry of the Upper and Lower Atmosphere, Academic Press, San Diego, 2000.

Grimmer, G., Jacob, J., and Noujack, K. W.: Profile of the polycyclic aromatic hydrocarbons from lubricating oils. Inventory by GC/MS-PAH in environmental materials, Part 1, Fresen. Z. Anal. Chem., 314, 13–19, 1983.

Herner, J. D., Ying, Q., Aw, J., Gao, O., Chang, D. P. Y., and Kleeman, M. J.: Dominant mechanism that shape the airborne particle size and composition distribution in central California, Aerosol Sci. Tech., 40, 827–844, 2006.

Hinds, W. C.: Aerosol Technology: Properties, Behavior, and Measurement of Airborne Particles, John Wiley & Sons, New York, 1999.

Huang, X. F., Yu, J. Z., He, L. Y., and Yuan, Z. B.: Water-soluble organic carbon and oxalate in aerosols at a coastal urban site in China: Size distribution characteristics, sources, and formation mechanisms, J. Geophys. Res.-Atmos., 111, D22212, doi:10.1029/2006JD007408, 2006.

Huebert, B. J., Bates, T., Russell, P. B., Shi, G. Y., Kim, Y. J., Kawamura, K., Carmichael, G., and Nakajima, T.: An overview of ACE-Asia: Strategies for quantifying the relationships between Asian aerosols and their climatic impacts, J. Geophys. Res.-Atmos., 108, 8663, doi:10.1029/2003JD003550, 2003.

Kanakidou, M., Seinfeld, J. H., Pandis, S. N., Barnes, I., Dentener, F. J., Facchini, M. C., Van Dingenen, R., Ervens, B., Nenes, A., Nielsen, C. J., Swietlicki, E., Putaud, J. P., Balkanski, Y., Fuzzi, S., Horth, J., Moortgat, G. K., Winterhalter, R., Myhre, C. E. L., Tsigaridis, K., Vignati, E., Stephanou, E. G., and Wilson, J.: Organic aerosol and global climate modelling: a review, Atmos. Chem. Phys., 5, 1053–1123, 2005, http://www.atmos-chem-phys.net/5/1053/2005/.

Kavouras, I. G. and Stephanou, E. G.: Particle size distribution of organic primary and secondary aerosol constituents in urban, background marine, and forest atmosphere, J. Geophys. Res.-Atmos., 107(D8), 4069, doi:10.1029/2000JD000278, 2002.

Keshtkar, H. and Ashbaugh, L. L.: Size distribution of polycyclic aromatic hydrocarbon particulate emission factors from agricultural burning, Atmos. Environ., 41, 2729–2739, 2007.

Kleeman, M. J. and Cass, G. R.: Effect of emissions control strategies on the size and com-

Size-distributions of *n*-hydrocarbons, PAHs and hopanes and their sources

G. Wang et al.

position distribution of urban particulate air pollution, Environ. Sci. Technol., 33, 177–189, 1999.

Kleeman, M. J., Schauer, J. J., and Cass, G. R.: Size and composition distribution of fine particulate matter emitted from wood burning, meat charbroiling, and cigarettes, Environ. Sci. Technol., 33, 3516–3523, 1999.

Kleeman, M. J., Riddle, S. G., and Jakober, C. A.: Size distribution of particle-phase molecular markers during a severe winter pollution episode, Environ. Sci. Technol., 42, 6469–6475, 2008.

Offenberg, J. H. and Baker, J. E.: Aerosol size distributions of polycyclic aromatic hydrocarbons in urban and over-water atmospheres, Environ. Sci. Technol., 33, 3324–3331, 1999.

Ohura, T., Amagai, T., Fusaya, M., and Matsushita, H.: Polycyclic aromatic hydrocarbons in indoor and outdoor environments and factors affecting their concentrations, Environ. Sci. Technol., 38, 77–83, 2004.

Oros, D. R. and Simoneit, B. R. T.: Identification and emission rates of molecular tracers in coal smoke particulate matter, Fuel, 79, 515–536, 2000.

Pierce, R. C. and Katz, M.: Dependency of polynuclear aromatic hydrocarbon content on size distribution of atmospheric aerosols, Environ. Sci. Technol., 9, 347–353, 1975.

Ramanathan, V. C., Kiehl, J. T., and Rosenfeld, D.: Aerosols, climate, and the hydrological cycle, Science, 294, 2119–2124, 2001.

Riddle, S. G., Robert, M. A., Jakober, C. A., Hannigan, M. P., and Kleeman, M. J.: Size distribution of trace organic species emitted from heavy-duty diesel vehicles, Environ. Sci. Technol., 42, 974–976, 2008.

Rogge, W. F., Hildemann, L. M., Mazurek, M., and Cass, G. R.: Sources of fine organic aerosol. 2. Noncatalyst and catalyst-equipped automobiles and heavy-duty diesel trucks, Environ. Sci. Technol., 27, 636–651, 1993a.

Rogge, W. F., Hildemann, L. M., Mazurek, M. A., and Cass, G. R.: Sources of fine organic aerosol. 4. Particulate abrasion products from leaf surfaces of urban plants, Environ. Sci. Technol., 27, 2700–2711, 1993b.

Seinfeld, J. H. and Pandis, S. N.: Atmospheric Chemistry and Physics, John Wiley & Sons, New York, 1998.

Seinfeld, J. H. and Pankow, J. F.: Organic atmospheric particulate material, Annu. Rev. Phys. Chem., 54, 121–140, 2003.

Simoneit, B. R. T., Sheng, G., Chen, X., Fu, J., Zhang, J., and Xu, Y.: Molecular marker study of

Size-distributions of *n*-hydrocarbons, PAHs and hopanes and their sources

G. Wang et al.

extractable organic matter in aerosols from urban areas of China, Atmos. Environ. A-Gen., 25, 2111–2129, 1991.

Simoneit, B. R. T., Kobayashi, M., Mochida, M., Kawamura, K., and Huebert, B. J.: Aerosol particles collected on aircraft flights over the northwestern Pacific region during the ACE-Asia campaign: Composition and major sources of the organic compounds, J. Geophys. Res.-Atmos., 109, D19S09, doi:10.1029/2004JD004565, 2004a.

Simoneit, B. R. T., Kobayashi, M., Mochida, M., Kawamura, K., Lee, M., Lim, H. J., Turpin, B. J., and Komazaki, Y.: Composition and major sources of organic compounds of aerosol particulate matter sampled during the ACE-Asia campaign, J. Geophys. Res.-Atmos., 109, D19S10, doi:10.1029/2004JD004598., 2004b.

Venkataraman, C., Lyons, J. M., and Friedlander, S. K.: Size distributions of polycyclic aromatic hydrocarbons and elemental Carbon. 1. Sampling, measurement methods, and source characterization, Environ. Sci. Technol., 28, 555–562, 1994.

Venkataraman, C., Negi, G., Brata Sardar, S., and Rastogi, R.: Size distributions of polycyclic aromatic hydrocarbons in aerosol emissions from biofuel combustion, J. Aerosol Sci., 33, 503–518, 2002.

Wang, G. H., Kawamura, K., Lee, S. C., Ho, K. F., and Cao, J. J.: Molecular, seasonal and spatial distributions of organic aerosols from fourteen Chinese cities, Environ. Sci. Technol., 40, 4619–4625, 2006.

Wang, G. H., Kawamura, K., Zhao, X., Li, Q. G., Dai, Z. X., and Niu, H. Y.: Identification, abundance and seasonal variation of anthropogenic organic aerosols from a mega-city in China, Atmos. Environ., 41, 407–416, 2007.

Yao, X., Lau, A. P. S., Fang, M., Chan, C. K., and Hu, M.: Size distributions and formation of ionic species in atmospheric particulate pollutants in Beijing, China: 2-dicarboxylic acids, Atmos. Environ., 37, 3001–3007, 2003.

Yu, J. Z., Yang, H., Zhang, H., and Lau, A. K. H.: Size distributions of water-soluble organic carbon in ambient aerosols and its size-resolved thermal characteristics, Atmos. Environ., 38, 1061–1071, 2004.

Zheng, M., Kester, D. R., Wang, F., Shi, X., and Guo, Z.: Size distribution of organic and inorganic species in Hong Kong aerosols during the wet and dry seasons, J. Geophys. Res.-Atmos., 113, D16303, doi:10.1029/2007JD009424, 2008.

Table 1. Sampling information and particle concentrations.

| | Urban (Baoji) | | Mountain (Mt. Tai) | | Marine (Okinawa Is.) |
	Winter	Spring	Winter	Summer	Spring
Date	11–14 Jan, 12–20 Feb 2008	12–24 Apr 2008	12–24 Jan 2008	22–28 Jun 2006	18 Mar–4 Apr 2008
Duration of each sample	4 d	4 d	4 d	7 d	3–5 d
Number of sample sets	3	3	3	1	5
TSP, $\mu g\,m^{-3}$	316±76	286±150	102±60	116	Not determined

Table 2. Concentrations of organic compounds in the total suspended particles (TSP) of the urban, mountain and marine atmosphere over East Asia, $\mathrm{ng\,m^{-3}}$.

| | Urban (Baoji) | | Mountain (Mt. Tai) | | Marine (Okinawa Is.) |
	Winter (n=3)	Spring (n=3)	Winter (n=3)	Summer[a] (n=1)	Spring (n=5)
I. _n_-Alkanes					
Octadecane (C_{18})	18±8.9	1.6±0.4	2.4±0.6	nd[b]	nd
Nonadecane (C_{19})	51±9.3	5.6±1.4	2.5±0.9	nd	nd
Icosane (C_{20})	95±24	9.4±1.2	3.4±1.3	0.2	nd
Henicosane (C_{21})	156±45	21±3.8	6.0±2.6	nd	0.27±0.02
Docosane (C_{22})	202±69	28±5.2	8.8±4.5	0.9	0.16±0.12
Tricosane (C_{23})	241±89	48±12	12±7.3	2.2	0.38±0.29
Tetracosane (C_{24})	203±78	57±17	11±7.8	2.2	0.44±0.35
Pentacosane (C_{25})	208±82	69±21	12±8.5	3.0	0.82±0.63
Hexacosane (C_{26})	121±45	50±17	9.5±7.4	2.6	0.79±0.65
Heptacosane (C_{27})	77±28	37±10	7.7±6.0	5.0	0.96±0.69
Octacosane (C_{28})	54±18	30±11	7.4±6.0	3.3	0.76±0.61
Nonacosane (C_{29})	61±24	27±7.5	7.9±6.3	8.2	0.69±0.53
Triacotane (C_{30})	30±9.3	19±7.0	4.8±3.9	2.6	0.42±0.32
Hentriacotane (C_{31})	90±34	37±16	16±13	5.6	1.4±1.0
Dotriacotane (C_{32})	20±6.2	13±4.9	3.4±2.8	1.9	0.26±0.19
Tritriacotane (C_{33})	39±14	20±6.2	7.5±6.2	1.9	0.50±0.36
Tetratriacotane (C_{34})	11±4.0	7.6±3.0	1.8±1.8	0.8	0.07±0.07
PentatriacotaneC_{35}	13±4.3	6.3±2.8	1.4±2.4	0.4	0.06±0.07
Hexatriacotane (C_{36})	6.6±3.2	2.5±1.1	0.3±0.6	0.3	nd
Subtotal	1698±568	487±145	126±88	41	7.9±6.1
II. PAHs					
Dibenzothiophene (DB)	2.3±0.8	0.3±0.1	1.1±0.7	nd	nd
Phenanthrene (Phe)	19±9.2	1.4±0.7	4.1±2.5	0.5	nd
Anthracene (Ant)	2.3±1.0	0.4±0.3	0.3±0.1	0.1	nd
Fluoranthene (Flu)	50±14	6.0±2.0	7.2±4.8	1.1	0.13±0.10
Pyrene (Pyr)	39±9.4	5.5±1.8	4.5±2.8	0.9	0.09±0.07
Benzo(b)fluorine (BF)	10±1.3	0.7±0.5	0.5±0.3	0.1	nd
Chrysene/Triphenylene (CT)	42±2.2	13±5.2	5.2±3.0	0.2	0.06±0.06
Benzo(b/k)fluoranthene (BbkF)	112±11	39±11	14±8.8	1.6	0.40±0.37
Benzo(e)pyrene (BeP)	29±2.5	9.6±2.4	3.1±2.3	1.0	0.05±0.05
Benzo(a)pyrene (BaP)	33±2.9	11±3.9	2.1±1.4	0.8	0.03±0.02
Perylene (Per)	8.3±1.0	3.3±1.1	0.3±0.2	0.1	nd
Indeno[123-cd]pyrene (IP)	39±4.6	16±5.0	2.4±1.9	1.1	0.07±0.06
Dibenz(a,h)anthracene (DBA)	15±1.8	2.9±0.7	0.9±0.8	0.2	nd
Benzo(ghi)perylene (BghiP)	34±3.8	15±4.3	2.5±1.9	1.0	0.05±0.04
Anthanthrene (Antha)	13±1.2	4.0±1.8	0.5±0.3	0.1	nd
Coronene (Cor)	34±9.9	14±5.4	3.0±2.5	0.6	0.03±0.02
Dibenzo(a,e)pyrene (DBP)	54±24	19±6.5	6.3±5.9	nd	0.03±0.03
Subtotal	536±80	161±39	58±42	9.2	0.65±0.60

Size-distributions of _n_-hydrocarbons, PAHs and hopanes and their sources

G. Wang et al.

Title Page

Abstract | Introduction

Conclusions | References

Tables | Figures

|◀ | ▶|

◀ | ▶

Back | Close

Full Screen / Esc

Printer-friendly Version

Interactive Discussion

Table 2. Continued.

	Urban (Baoji)		Mountain (Mt. Tai)		Marine (Okinawa Is.)
	Winter (n=3)	Spring (n=3)	Winter (n=3)	Summer[a] (n=1)	Spring (n=5)
III. Hopanes					
17α(H)-22,29,30-trisnorhopane (C$_{27\alpha}$)	6.5±2.4	1.3±0.2	0.07±0.03	nd	nd
17β(H)-22,29,30-trisnorhopane (C$_{27\beta}$)	7.8±3.1	1.5±0.1	0.01±0.02	nd	nd
17α(H),21β(H)-30-norhopane (C$_{29\alpha\beta}$)	10±3.4	3.7±0.4	0.29±0.06	0.05	nd
17β(H),21α(H)-30-norhopane (C$_{29\beta\alpha}$)	13±5.3	2.6±0.4	0.10±0.09	nd	nd
17α(H),21β(H)-30-hopane (C$_{30\alpha\beta}$)	6.8±2.3	3.6±0.4	0.36±0.14	0.11	nd
17β(H),21α(H)-30-hopane (C$_{30\beta\alpha}$)	7.7±3.2	1.8±0.2	0.08±0.01	nd	nd
17α(H),21β(H)-22S-homohopane (C$_{31\alpha\beta}$S)	1.6±0.5	1.2±0.2	0.06±0.01	0.01	nd
17α(H),21β(H)-22R-homohopane (C$_{31\alpha\beta}$R)	3.3±1.3	1.2±0.1	0.07±0.06	0.01	nd
17β(H),21α(H)-30-homohopane (C$_{31\beta\alpha}$)	3.9±1.5	0.9±0.1	0.01±0.01	nd	nd
17α(H),21β(H)-22S-bishomohopane (C$_{32\alpha\beta}$S)	1.2±0.3	1.1±0.2	0.03±0.04	0.03	nd
17α(H),21β(H)-22R-bishomohopane (C$_{32\alpha\beta}$R)	2.6±0.7	1.1±0.1	0.01±0.01	nd	nd
Subtotal	65±24	20±2.4	1.1±0.1	0.21	nd

[a] Sum of compounds in particles with a diameter less than 9.0 µm.
nd: not detected

Table 3. TSP-equivalent concentrations (ng m^{-3}) of biomarkers and their diagnostic ratios.

	Urban Winter (n=3)	Urban Spring (n=3)	Mountain Winter (n=3)	Mountain Summer (n=1)	Marine Spring (n=5)	Sources Gasoline	Sources Diesel	Coal
I. *n*-Alkanes								
Plant wax[a]	228±87	74±21	25±18	13	2.3±1.7			
Fossil fuel[a]	1470±482	413±124	101±71	28	5.6±4.2			
WNA%[b]	13±1.0	15±0.2	19±4.0	31	30±4.3			
CPI[c]	1.2±0.0	1.3±0.0	1.3±0.2	1.8	1.7±0.2			
II. PAHs								
BeP/(BeP+BaP)	0.5±0.0	0.5±0.0	0.6±0.0	0.6	0.6±0.0			
IP/BghiP	1.2±0.1	1.1±0.3	1.9±0.1	1.0	1.4±0.1	0.2[d]	0.5[d]	1.3[d]
BghiP/BeP	1.2±0.0	1.5±0.1	0.8±0.2	1.0	0.9±0.1	2.0[e]		0.8[e]
III. Hopanes								
$C_{29\alpha\beta}/C_{30\alpha\beta}$	1.5±0.0	1.0±0.0	0.9±0.2	0.5		0.6–0.7[f]	0.4[f]	0.6–2.0[g]
$C_{31\alpha\beta}$ [S/S+R]	0.3±0.0	0.5±0.0	0.5±0.2	0.6		0.6[f]	0.5[f]	0.1–0.4[g]
$C_{32\alpha\beta}$ [S/S+R]	0.3±0.0	0.5±0.0				0.6[f]	0.6[f]	0.2–0.4[g]

[a] Plant wax *n*-alkanes: calculated as the excess odd homologues-adjacent even homologues average and the difference from the total *n*-alkanes is the fossil fuel-derived amount (Simoneit et al., 1991; Simoneit et al., 2004b);

[b] WNA%: wax *n*-alkanes percentage, calculated as $\sum C_n - 0.5(C_{n-1}+C_{n+1})/\sum$ *n*-alkanes (Simoneit et al., 1991; Kavouras and Stephanou, 2002);

[c] CPI, carbon preference index, $CPI_1 = \sum C_{19} - C_{35}/\sum C_{18} - C_{34}$;

[d] Grimmer et al. (1983);

[e] Ohura et al. (2004);

[f] Rogge et al. (1993a);

[g] Oros and Simoneit (2000).

Table 4. Concentrations of *n*-alkanes, PAHs and hopanes in each stage of the impactor samples from the urban mountain and marine atmosphere over East Asia.

| | | | | Size range (µm) | | | | | |
	<0.4	0.4–0.7	0.7–1.1	1.1–2.1	2.1–3.3	3.3–4.7	4.7–5.8	5.8–9.0	>9.0
					Urban (Baoji)				
I. Winter (*n*=3)									
$\sum n-$Alkanes, ng m^{-3}	217	321	486	437	103	54	29	26	25
Cumulative percentage, %	13	32	60	86	92	95	97	99	100
$\sum$PAHs, ng m^{-3}	51	106	186	157	20	7.2	3.4	3.2	2.9
Cumulative percentage, %	9.5	29	64	93	97	98	99	99	100
$\sum$Hopanes, ng m^{-3}	9.2	13	20	15	2.7	1.5	0.7	0.9	0.9
Cumulative percentage, %	14	35	66	90	94	96	97	99	100
II. Spring (*n*=3)									
$\sum n-$Alkanes, ng m^{-3}	81	105	117	74	30	23	14	21	23
Cumulative percentage, %	17	38	62	77	83	88	91	95	100
$\sum$PAHs, ng m^{-3}	29	52	49	23	3.8	1.9	0.9	1.3	1.3
Cumulative percentage, %	18	50	80	94	97	98	98	99	100
$\sum$Hopanes, ng m^{-3}	4.0	4.3	4.4	3.4	1.0	0.9	0.5	0.9	1.0
Cumulative percentage, %	20	41	63	80	84	89	91	95	100
					Mountain (Mt. Tai)				
I. Winter (*n*=3)									
$\sum n$-Alkanes, ng m^{-3}	9	14	32	45	12	5	3	3	3
Cumulative percentage, %	7	18	43	80	89	93	95	98	100
$\sum$PAHs, ng m^{-3}	2	7	17	23	6	1	0.5	0.4	0.4
Cumulative percentage, %	3	16	45	85	95	98	99	99	100
$\sum$Hopanes, pg m^{-3}	83	170	309	327	94	49	13	23	18
Cumulative percentage, %	8	23	52	82	91	95	96	98	100
II. Summer (*n*=1)									
$\sum n$-Alkanes, ng m^{-3}	2	8	12	8	2	2	2	4	n.a.[a]
Cumulative percentage, %	5	26	55	75	80	86	91	100	n.a.
$\sum$PAHs, ng m^{-3}	0.5	2	3	2	0.7	0.4	0.3	0.3	n.a.
Cumulative percentage, %	5.6	24	61	83	90	94	97	100	n.a.
$\sum$Hopanes, pg m^{-3}	20	34	51	23	0	19	7	24	n.a.
Cumulative percentage, %	11	30	59	72	72	83	87	100	n.a.
					Marine (Okinawa Is.)				
I. Spring (*n*=5)									
$\sum n$-Alkanes, ng m^{-3}	0.7	0.6	2	2	0.8	0.5	0.2	0.1	1
Cumulative percentage, %	8	15	39	65	75	82	84	86	100
$\sum$PAHs, pg m^{-3}	23	38	209	292	68	14	3	2	0
Cumulative percentage, %	3.5	9.4	42	87	97	99	100	100	100

[a] n.a.: not available. Size fractions (>9.0 µm) of the mountain summer samples sets were not analyzed.

Title Page

Abstract | Introduction

Conclusions | References

Tables | Figures

|◄ | ►|

◄ | ►

Back | Close

Full Screen / Esc

Printer-friendly Version

Interactive Discussion

Table 5. Geometric mean diameter (GMD, µm)[a] of the biomarkers calculated for the fine (<2.1 µm) and coarse (≥2.1 µm) particles and the whole range of impactor particle sizes (total) in the urban, mountain and marine atmospheres over East Asia.

| | Urban (Baoji) | | | | | | Mountain (Mt. Tai) | | | | | | Marine (Okinawa Is.) | | |
| | Winter (n=3) | | | Spring (n=3) | | | Winter (n=3) | | | Summer (n=1) | | | Spring (n=5) | | |
	Fine	Coarse	Total	Fine	Coarse	Total	Fine	Coarse	Total	Fine	Coarse	Total	Fine	Coarse	Total
I. Particles	0.93±0.04	4.34±0.33	1.47±0.07	0.85±0.04	4.73±0.22	1.85±0.12	0.82±0.12	4.63±0.17	1.70±0.08	0.65	5.56	2.49	nd[b]	nd	nd
II. n-Alkanes															
∑n-alkanes	0.77±0.03	3.67±0.14	0.94±0.02	0.64±0.02	4.26±0.18	0.94±0.10	0.89±0.16	3.83±0.46	1.13±0.21	0.82	4.87	1.28	0.91±0.09	3.88±0.43	1.28±0.07
Fossil fuel[c]	0.76±0.03	3.80±0.38	0.91±0.02	0.64±0.02	4.22±0.16	0.90±0.10	0.89±0.16	3.70±0.17	1.11±0.23	0.84	4.62	1.05	0.90±0.10	3.85±0.50	1.24±0.13
Plant wax[c]	0.89±0.05	3.54±0.08	1.15±0.05	0.69±0.02	4.38±0.27	1.16±0.13	0.89±0.17	3.91±0.68	1.24±0.12	0.75	5.03	1.98	0.93±0.08	3.92±0.23	1.41±0.15
III. PAHs															
∑PAHs	0.83±0.05	3.47±0.18	0.91±0.06	0.63±0.06	3.81±0.18	0.69±0.08	0.99±0.11	3.26±0.17	1.14±0.17	0.85	3.93	1.10	1.20±0.16	3.07±0.19	1.35±0.09
3,4-ring	0.86±0.03	3.72±0.18	1.01±0.05	0.68±0.07	4.14±0.16	0.84±0.10	1.01±0.09	3.41±0.20	1.23±0.17	0.91	3.95	1.26	1.22±0.11	3.22±0.25	1.40±0.09
5,6-ring	0.82±0.06	3.19±0.20	0.87±0.06	0.62±0.06	3.59±0.12	0.66±0.07	0.97±0.12	2.98±0.08	1.07±0.18	0.82	3.91	1.03	1.18±0.22	2.93±0.23	1.34±0.15
IV. Hopanes															
∑Hopanes	0.74±0.03	3.70±0.33	0.86±0.01	0.62±0.03	4.38±0.23	0.85±0.04	0.90±0.20	3.37±0.32	1.15±0.47	0.69	5.58	1.25	nd	nd	nd
$C_{29\alpha\beta}$	0.74±0.03	3.82±0.36	0.88±0.01	0.60±0.03	4.49±0.22	0.86±0.06	0.82±0.20	3.31±0.30	1.14±0.49	0.71	3.98	0.87	nd	nd	nd
$C_{30\alpha\beta}$	0.73±0.03	3.99±0.37	0.93±0.01	0.60±0.02	4.52±0.16	0.92±0.07	0.90±0.19	3.50±0.48	1.26±0.54	0.67	5.53	1.28	nd	nd	nd

[a] $\log \text{GMD} = (\sum C_i \log Dp_i) / \sum C_i$, where C_i is the concentration of compound in size i and Dp_i is the geometric mean particle diameter collected on stage i (Hinds, 1999);

[b] Not detected;

[c] Plant wax means n-alkanes derived from plant wax, and fossil fuel means n-alkanes derived from fossil fuel emissions (for detailed calculations see Table 3).

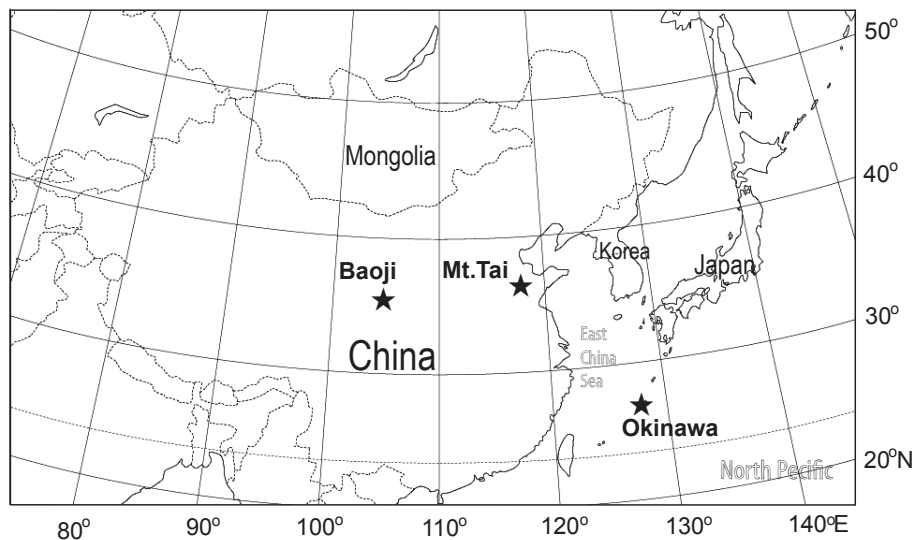**Fig. 1.** A map showing locations of the sampling sites and their surroundings in East Asia.

Title Page

Abstract | Introduction

Conclusions | References

Tables | Figures

◄◄ | ►►

◄ | ►

Back | Close

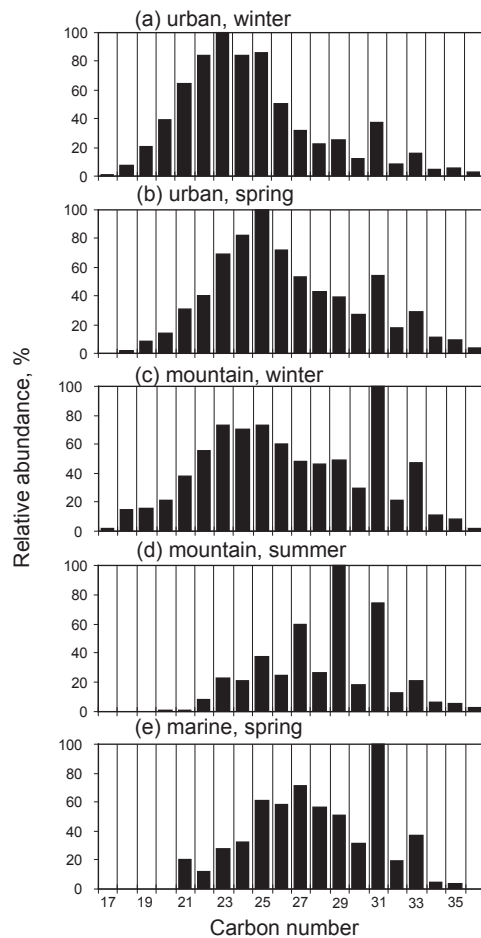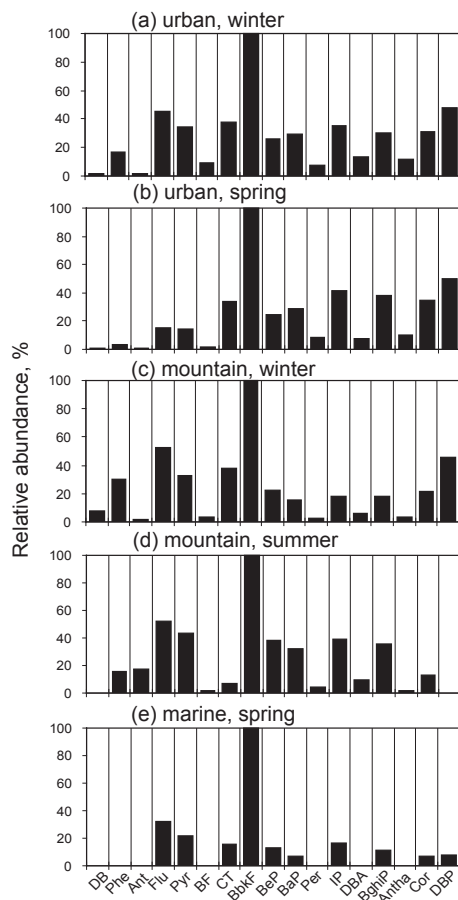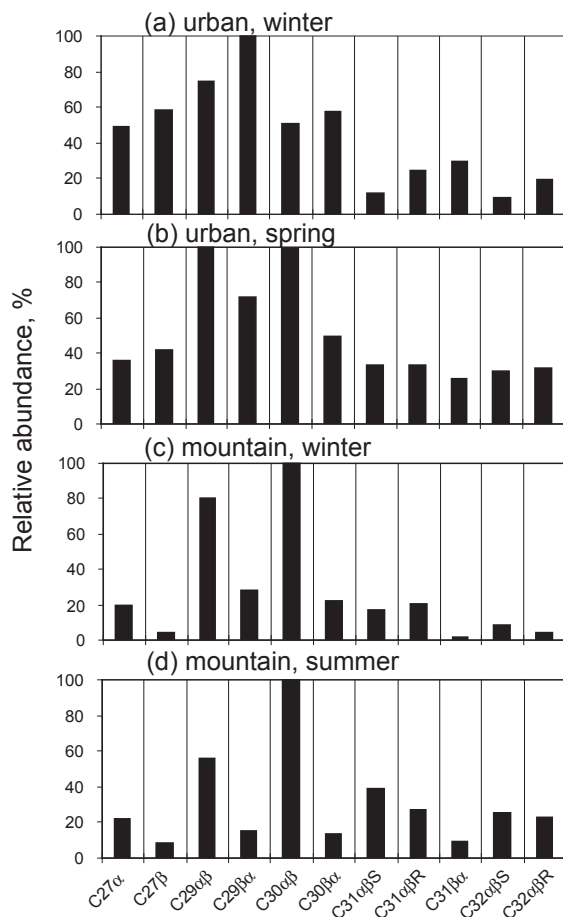Full Screen / Esc

Printer-friendly Version

Interactive Discussion

Fig. 2. Molecular distributions of TSP-associated *n*-alkanes in the urban, mountain and marine aerosol samples during different seasons.

Fig. 3. Molecular distributions of TSP-associated PAHs in the urban, mountain and marine aerosol samples during different seasons (for abbreviation, see Table 2).

Fig. 4. Molecular distributions of TSP-associated hopanes in the urban, mountain and marine aerosol samples during different seasons (for abbreviation, see Table 2).

Full Screen / Esc

Printer-friendly Version

Interactive Discussion
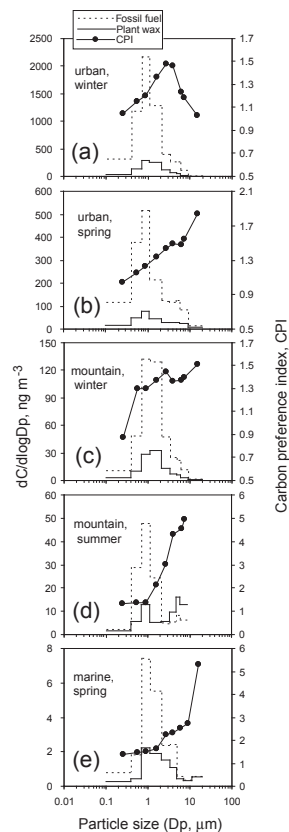
Fig. 5. Size distributions of fossil fuel- and plant wax- derived *n*-alkanes and CPI values of total *n*-alkanes in the urban, mountain and marine aerosols during different seasons. Plant wax derived *n*-alkanes are calculated as the excess odd carbon-numbered homologues-adjacent even carbon-numbered homologues average and the difference from the total *n*-alkanes is defined as the fossil fuel-derived *n*-alkanes (Simoneit et al., 1991; Simoneit et al., 2004b).
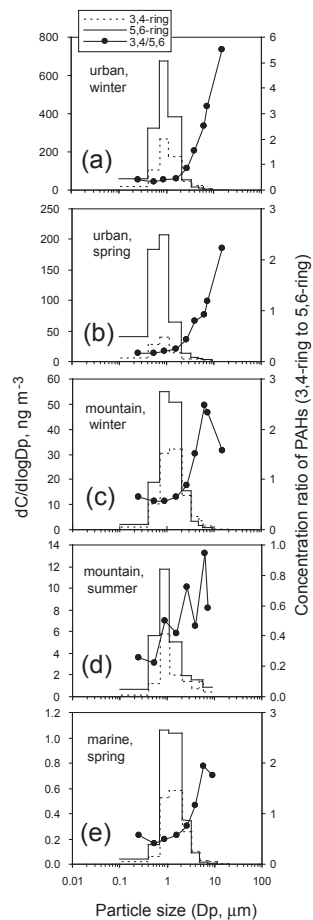
Fig. 6. Size distributions of PAHs in the urban, mountain and marine atmosphere during different seasons.

Title Page

Abstract | Introduction

Conclusions | References

Tables | Figures

◄ | ►►

◄ | ►

Back | Close

Full Screen / Esc

Printer-friendly Version
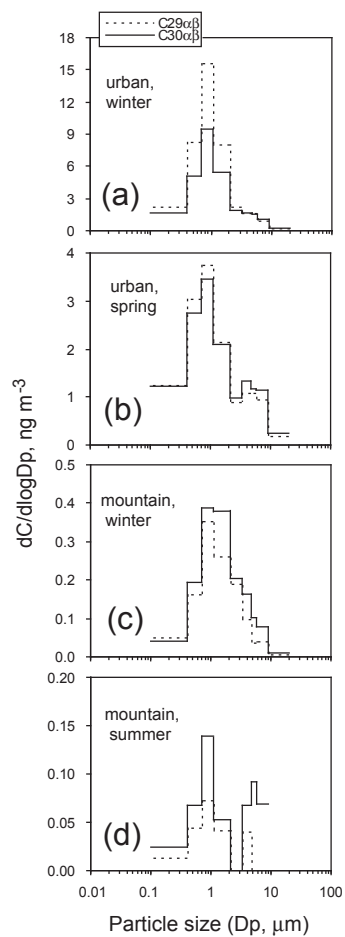
Interactive Discussion

Fig. 7. Size distributions of hopanes ($C_{29\alpha\beta}$ and $C_{30\alpha\beta}$) in the urban, mountain and marine atmosphere during different seasons.

Title Page

Abstract	Introduction
Conclusions	References
Tables	Figures

|◄   ►|

◄   ►

Back   Close

Full Screen / Esc

Printer-friendly Version

Interactive Discussion